Journal of
Water & Climate Change

IWA PUBLISHING

Journal of Water and Climate Change Vol 15 No 2, 305 doi: 10.2166/wcc.2023.459

Improvement of daily pan-evaporation calculation in arid and semi-arid regions by limited climatic data

Mehdi Mohammadi, Meysam Salarijazi *, Khalil Ghorbani and Amir-Ahmad Dehghani

Department of Water Engineering, Faculty of Water and Soil Engineering, Gorgan University of Agricultural Sciences and Natural Resources, Gorgan, Golestan Province, Iran
*Corresponding author. E-mail: meysam.salarijazi@gau.ac.ir

MS, 0000-0001-9010-1988

ABSTRACT

In this study, 14 equations have been investigated to calculate pan-evaporation in arid and semi-arid regions (based on the De Martonne aridity index). Two indicators i.e. nRMSE and MBE, were used to analyze the results. The Kohler -Nordonson -Fox (K -N -F) (1955) equation, on the one hand, is more precise than other original equations and, on the other hand, is one of the equations that has less impact from the improving process and, in other words, has a higher consistency compared to other equations in arid and semi-arid regions. Three improved equations, including improved K -N -F (1955), improved Linacer (1994), and improved Kohler (1954), have better precision in calculating the pan-evaporation compared to the other equations. According to the mathematical form of these three equations, this finding shows the importance of temperature, relative humidity, and wind velocity in arid and semi-arid regions. The improved Linacer (1954) equation had low precision in high-humidity regions, emphasizing relative humidity in calculating pan-evaporation in arid and semi-arid regions. Among 14 equations, more precisions have been from the category of improved equations, so it becomes clear that the empirical mathematical equations must be improved specifically for arid and semi-arid regions.

Key words: empirical equation, free water surface evaporation, humidity, optimization, spatial analysis, temperature

HIGHLIGHTS

- Fourteen equations have been investigated to calculate pan-evaporation in arid and semi-arid regions.
- The K–N–F (1955) equation has a higher consistency compared to other equations in arid and semi-arid regions.
- The improved K–N–F (1955), improved Linacre (1994), and improved Kohler (1954) have better precision in calculating the pan-evaporation compared to the other equations.

1. INTRODUCTION

Evaporation is an essential component of the hydrological cycle and is critical in hydrological studies (Adnan *et al.* 2019). The fundamental hydrological component leads to the fact that, in most cases, a large part of the water due to precipitation is out of reach (Flammini *et al.* 2018; Sebbar *et al.* 2019). Calculating the amount of evaporation in arid and semi-arid regions is of great interest (Yaseen *et al.* 2020). In arid regions, evaporation occurs with much greater intensity; therefore, the importance of this component is significantly increased (Majidi *et al.* 2015). One of the most critical problems for lakes, wetlands, and other water bodies in arid and semi-arid regions is the evaporation process, which significantly affects the water available for environmental needs (Alsumaiei 2020). An evaporation pan is the best-known way to record the amount of evaporation from the surface of open water (Jones 2018). In most climatic stations worldwide, evaporation pans are installed in various mathematical forms to record the amount of evaporation (Patle *et al.* 2020). The costs of setting up and maintaining climatic data recorders are high. Therefore, the number and dispersion of these stations are limited (Mohammadi *et al.* 2023). Using mathematical equations that improve with the recorded data leads to empirical mathematical equations (Dlouhá *et al.* 2021). Applying these equations makes it possible to calculate different components in regions where data are not recorded (Majhi *et al.* 2020). Different mathematical modeling methods such as Artificial Neural Network (ANN) (Seifi & Soroush 2020; Dehghanipour *et al.* 2021), Adaptive Neuro-Fuzzy Inference Systems (ANFIS) (Adnan *et al.* 2019), K-Nearest

Neighbors (KNN) (Yamaç 2021), and Support Vector Regression (SVR) (Guan *et al.* 2020) by different researchers to calculate surface water evaporation have been taken into consideration. Assessment of the results of these studies reveals that such new models provide more precise calculations than empirical mathematical equations (Kumar *et al.* 2021). The practical and engineering applications aspect is a significant limitation in using these models.

Considering several features, the equations presented for calculating evaporation can have practical and engineering applications: (a) developed for a specific climate, (b) the equation presented is clear and straightforward, and (c) the required data are selected from those recorded in most climatic stations. Most research has been based on the calculation of evaporation from open water. The equations for calculating evaporation from open water can be categorized differently (McMahon *et al.* 2013). McMahon *et al.* (2016) considered the equations for calculating evaporation as different categories. These categories include temperature, energy balance, radiation temperature, miscellaneous, and mass transfer. The equations presented to calculate evaporation from open water are various. A major drawback to applying most of these equations is access to relevant data in most regions. Most open water evaporation data have a limited recorded period. These data have been recorded in a few regions, and this is a serious problem to consider spatial variations. Also, recording such data by researchers requires a lot of cost and time. These limitations practically lead to the inability to study these equations in different climatic conditions and spatial variations with long-term data. In addition, open water involves a wide range of complexities because it involves evaporation from deep to shallow lakes with limited to wide surface area. Pan-evaporation data do not include the stated limitations, making it possible to consider standard data for studies. The presented equations for calculating the evaporation from open water are more varied than the pan-evaporation. A remarkable number of equations presented to calculate pan-evaporation depend on having a variety of data. Lack of access to radiation and other data in most parts of the world makes it impossible to use such equations. A few equations have been proposed to calculate pan-evaporation using finite climatic data. These equations have been studied in limited studies. Arid and semi-arid regions typically have lower wind velocity, lower relative humidity, and higher temperatures than other regions, which cause fundamental changes in the amount of evaporation. It is essential to pay attention to the precision and improvement of the equations for calculating pan-evaporation from these regions considering the particular climatic conditions of arid and semi-arid regions.

A review of the literature on calculating pan-evaporation in arid and semi-arid regions concluded that the studies had various shortcomings. Some of these defects are not applying some conditions as follows: (1) using components with a remarkable range of variability. (2) Focus on straight-mathematical form equations. (3) Use of data specific to arid and semi-arid regions. (4) Use of climatic components, which are often available. The main purpose of this study is to analyze and develop equations to calculate pan-evaporation in arid and semi-arid regions. The authors consider practical aspects of this study. Therefore, the following features are considered to select equations and study regions and climatic components in this manuscript: (A) the equations have a simple mathematical form so that they do not have high complexity in improving the achievement of suitable answers. (B) The climatic components used are those that are recorded in most regions. (C) Use many different recorded data series. (D) In the mathematical form of these equations, the characteristics of arid and semi-arid regions should be considered. (E) Equations should have different mathematical forms. (F) The original equation should be presented with a focus on pan-evaporation. (G) The range of changes in climatic components is wide. It seems that no study has been done considering all the cases mentioned together and specifically for arid and semi-arid regions, and it is the study's novelty. Although the maximum series and available data were used in this study, data from different parts of the world could increase its generalizability. However, the lack of access to the required data from other parts of the world is limited for this research.

2. MATERIAL AND METHODS

2.1. Aridity index

The definition of aridity can be considered the degree to which a climate lacks sufficient, life-promoting moisture, and is the opposite of humidity in the climate sense of the term (American Meteorological Society 2006). The higher value of the aridity index in a region equals more variability of the water resources (Costa & Soares 2012). More dry periods over a region result from increased aridity (Deniz *et al.* 2011). Different indices, including United Nations Environmental Programme (UNEP) (Zarei & Mahmoudi 2021), Mezentsev's moisture ratio (Nyamtseren *et al.* 2018), de Martonne (Pellicone *et al.* 2019), and Selyaninov's hydrothermal coefficient (Vlăduţ & Licurici 2020), were developed for aridity studies. This study applied the de Martonne index to select the recorded data series of arid and semi-arid regions. The I_{DM} (index of de Martonne) was

calculated by the following equation (Zhang *et al.* 2019):

$$I_{DM} = \frac{P}{T + 10}$$

In this equation, P and T are annual mean precipitation (mm) and annual mean temperature (°C), and therefore, the unit of I_{DM} is (mm/°C) (Alekseev *et al.* 2020). The details of climatic classification are presented in Table 1 (Croitoru *et al.* 2013).

2.2. Studied regions

The necessary components to determine the aridity index were extracted by assessing different recorded data series. Based on this, recorded data series located in arid and semi-arid regions were selected. Large regions of Iran are located in the arid and semi-arid regions (Salarijazi *et al.* 2023). The spatial distribution of the recorded data series is presented in Figure 1. As shown in Figure 1, except for a limited region of northern Iran, other parts of Iran are mainly located in arid and semi-arid regions (Modabber-Azizi *et al.* 2023). The recorded data series selected for this study includes 34 climatic stations in the range of longitude 45° 3′19 ″to 60° 54′ 1″ and latitude 25° 43′11 ‘to 37° 39′ 30″.

2.3. Data sets

The data series used in this research has been recorded in climatic stations. The characteristics of this recorded data series are presented in Table 2. These stations have long-term recorded data series of acceptable quality and quantity. Data preparation steps include data access, sorting and arrangement, data defects, identification and investigation of extreme data behavior, selection of corrected recorded data series, determination of aridity index for recorded data series, and series detection belonging to arid and semi-arid regions, and the final selection of the studied recorded data series. Details of these steps are provided in the mathematical form of a flowchart in Figure 2. Many climatic stations around the world use class A evaporation pans. This evaporation pan is the standard pan for all evaporation stations in Iran. It is 121 cm in diameter and 25 cm in depth. This pan is installed slightly above ground on the wood firm (Shammout *et al.* 2018).

Figure 3 shows the scattergram plots of climatic components for the recorded data series of arid and semi-arid regions. Attention to these plots reveals that the climatic components in this study have a great range and various distribution patterns. This feature is an advantage in the recorded data series because it increases the reliability of the computational results. Evaporation and temperature data show high values of these two climatic components in the recorded data series. Relative humidity data also indicate a pattern of change within the year. A weak pattern of within-the-year changes in wind velocity can also be detected.

2.4. Empirical equations of pan-evaporation

Pan-evaporation data are not available in many regions. Also, the available recorded data series have a limited dataset with a significant gap in many cases. These limitations have led researchers to study empirical mathematical equations for calculating pan-evaporation (Chaudhari *et al.* 2012). These researches studies examine and assess the discovery of the relationship between evaporation and climatic components in the form of mathematical equations (Ghumman *et al.* 2020). Several equations for calculating pan-evaporation have been developed based on applying the radiation component (Chen *et al.* 2019). These equations are limited because the radiation component is not recorded in many stations that record climatic

Table 1 | Type of climate according to the de Martonne aridity index (Croitoru *et al.* 2013)

Climate type	I_{DM} values
Arid	$I_{DM} \leq 10$
Semi-arid	$10 \leq I_{DM} < 20$
Mediterranean	$20 \leq I_{DM} < 24$
Semi-humid	$24 \leq I_{DM} < 28$
Humid	$28 \leq I_{DM} < 35$
Very humid	$35 \leq I_{DM} < 55$
Extremely humid	$I_{DM} > 55$

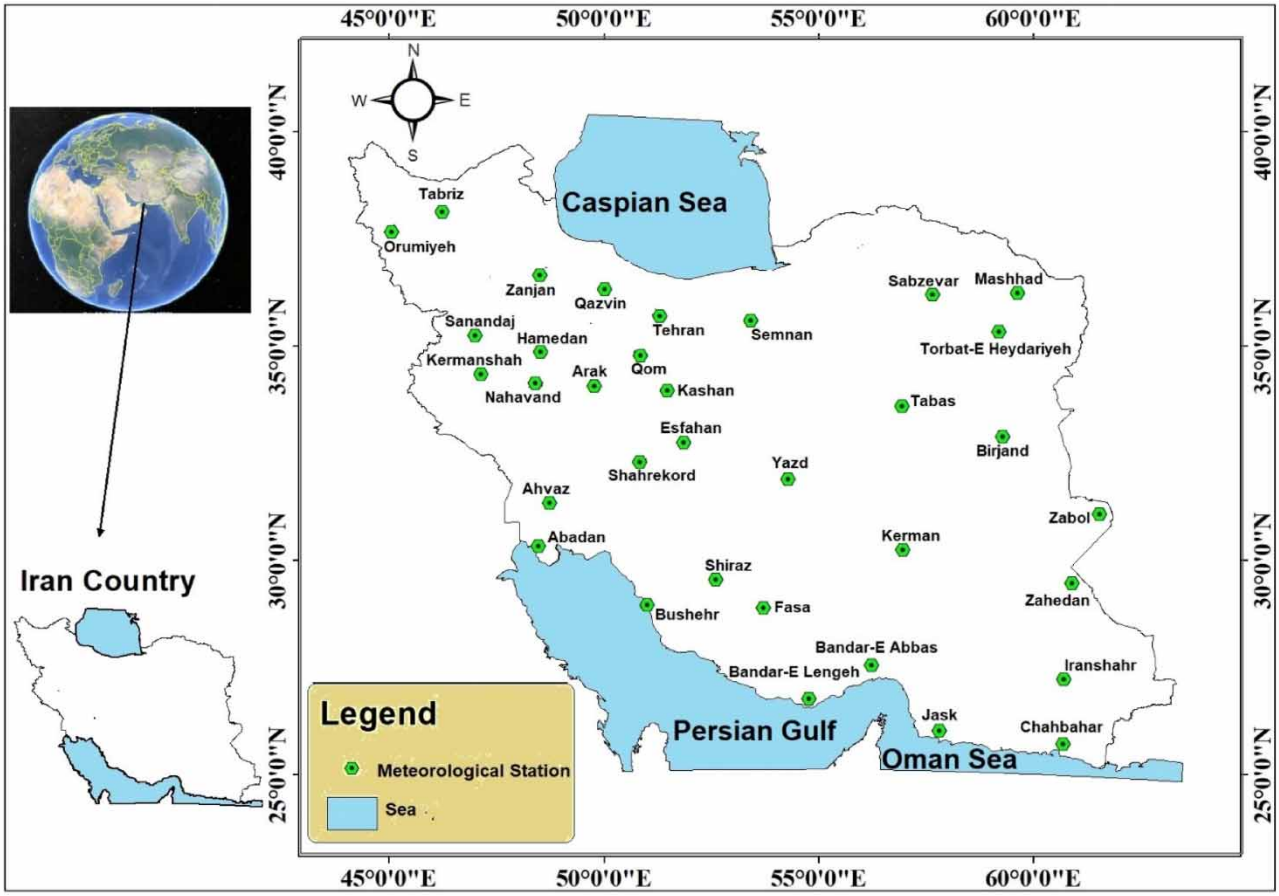

Figure 1 | Location of climatic stations in arid and semi-arid regions.

components. In this study, the equations developed to calculate evaporation using a limited number of climatic components are considered because these equations are more applicable than radiation-based equations.

2.4.1. Trabert (1896) equation

The Trabert (1896) equation has a long history in calculating evaporation (Lu *et al.* 2018). This equation uses the climatic components of temperature, relative humidity, and wind velocity to calculate evaporation. It has only one coefficient (Guan *et al.* 2020). The Trabert equation also considers the relationship between wind velocity and evaporation to be radical.

$$E = \alpha_{22} \sqrt{V} (e_s - e_d)$$

E is the calculated evaporation (mm/day); V is the wind velocity at the height of 2 m above the ground (m/s), $(e_s - e_d)$ is the VPD (kPa), and finally the $\beta_1 = 0.3075$ is the coefficient of the equation.

2.4.2. Antal (1973) equation

Antal (1973) presents this equation, and the inputs of the equation are the climatic components of temperature and relative humidity. The amount of VPD is also calculated as the second input of the equation using these two components (Antal 1973; Basnyat 1987). This equation assumes that the relationship between the input components and the amount of evaporation is a power relationship.

$$E = \beta_2 (e_s - e_d)^{\beta_3} \left(\beta_4 + \frac{T}{\beta_5}\right)^{\beta_6}$$

Table 2 | Characteristics of data series recorded in arid and semi-arid regions

Station name	Longitude	Latitude	Aridity index	Elevation	Station code
Tabriz	38° 17′ 18″	46° 14′ 31″	13	1,361	NW1
Orumiyeh	37° 39′ 30″	45° 3′ 19″	16	1,328	NW2
Sanandaj	35° 15′15″	47° 0′ 52″	18	1,373.4	W1
Kermanshah	31° 21′ 7″	47° 9′ 11″	17	1,318.5	W2
Ahvaz	31° 20′ 39″	48° 44′ 39″	5.6	22.5	SW1
Abadan	30° 20′ 27″	48° 29′ 13″	4.2	6.6	SW2
Zanjan	36° 39′ 37″	48° 31′ 18″	14	1,659.4	C1
Qazvin	36° 19′ 9″	50° 1′ 12″	13	1,279.1	C2
Hamedan	34° 52′ 9″	48° 32′ 4″	15	1,740.8	C3
Nahavand	34° 8′ 36″	48° 24′ 43″	4.7	1,677.8	C4
Arak	34° 4′ 18″	49° 46′ 59″	14	1,702.8	C5
Qom	34° 46′ 28″	50° 51′ 19″	4.7	879.1	C6
Tehran	35° 41′ 35″	51° 18′ 33″	8.4	1,191	C7
Semnan	35° 35′ 17″	53° 25′ 16″	4.8	1,127	C8
Kashan	33° 58′ 1″	51° 28′ 50″	4.4	955	C9
Esfahan	32° 44′ 39″	51° 51′ 47″	4.1	1,551.9	C10
Shahrekord	32° 14′ 39″	50° 50′ 21″	14	2,048.9	C11
Yazd	31° 54′ 14″	54° 17′ 21″	1.9	1,230.2	C12
Shiraz	29° 33′ 40″	52° 36′ 18″	12	1,488	C13
Fasa	28° 53′ 57″	53° 43′ 10″	9.3	1,268	C14
Kerman	30° 15′ 20″	56° 47′ 42″	5.2	1,754	C15
Tabas	33° 36′ 11″	56° 57′ 2″	2.4	711	C16
Bushehr	28° 58′ 26″	51° 0′ 28″	7.3	9	S1
Bandar-E-Lengeh	26° 46′ 58″	54° 46′ 26″	3.5	22.7	S2
Bandarabbas	27° 33′ 25″	56° 13′ 51″	4.6	9.8	S3
Jask	26° 2′ 23″	57° 48′ 27″	3.4	5.2	S4
Chahbahar	25° 43′ 11″	60° 41′ 13″	3.1	8	SE1
Iranshahr	27° 13′ 45″	60° 43′ 5″	2.8	591.1	SE2
Zahedan	29° 28′ 19″	60° 54′ 1″	2.9	1,370	E1
Zabol	31° 5′ 18″	61° 32′ 35″	1.6	489.2	E2
Birjand	32° 53′ 26″	59° 16′ 59″	6	1,491	E3
Torbat-E Heydariyeh	35° 19′ 12″	59° 12′ 20″	10	1,451	NE1
Mashhad	36° 14′ 11″	59° 37′ 51″	10	999.2	NE2
Sabzevar	36° 12′ 25″	58° 37′ 57″	6.6	962	NE3

In this equation, E is the calculated pan-evaporation (mm/day); $(e_s - e_d)$ is the VPD and its unit is millibars of mercury; T is the average daily temperature (°C). Also $\beta_2 = 1.1$, $\beta_3 = 0.7$, $\beta_4 = 1$, $\beta_5 = 273$, $\beta_6 = 4.8$ are the coefficients of the equation.

2.4.3. Linacre (1977) equation

This equation was developed by Linacre (1977), which uses only temperature among the climatic components and differs from other equations in this respect (Althoff *et al.* 2020). Another notable feature of this equation is the integration of geographical components to calculate evaporation so that the two components (latitude and elevation) are among the inputs

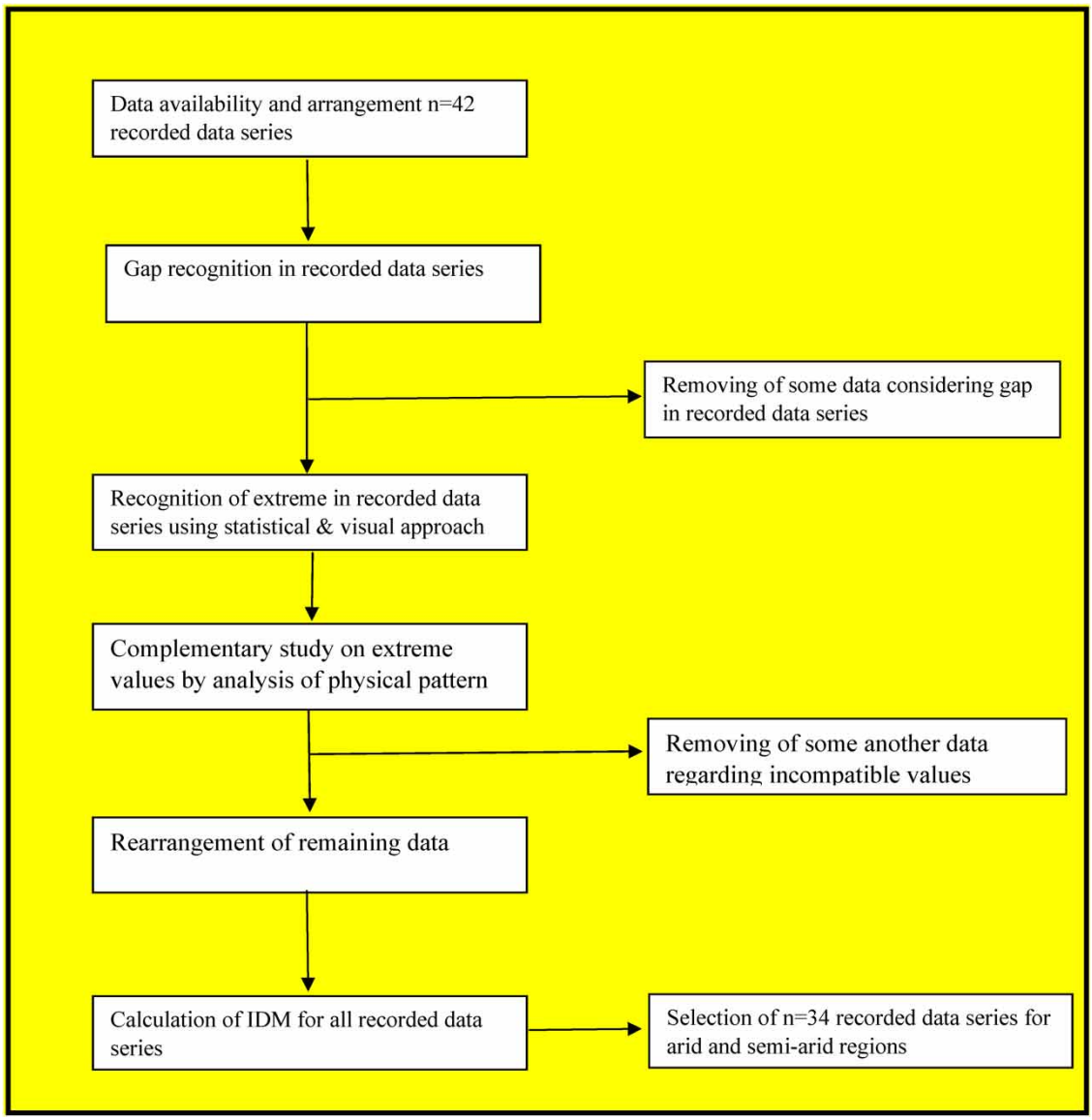

Figure 2 | Data preprocessing flowchart for studied arid and semi-arid regions.

to this equation (Linacre 1977).

$$E = \frac{\left[\beta_7 \left(\frac{(T + \beta_8 H)}{(\beta_9 - L) + \beta_{10}(T - T_d)}\right)\right]}{(\beta_{11} - T)}$$

E is the calculated pan-evaporation (mm/day); T is the average daily air temperature (°C), H is the elevation of the area (desired station) from the seawater level (m); L is the latitude of the location (°), T_d is the dew point temperature (°C); and $\beta_7 = 700$, $\beta_8 = 0.006$, $\beta_9 = 100$, $\beta_{10} = 15$, $\beta_{11} = 80$ are coefficients of the Linacre (1977) equation.

2.4.4. K–N–F (1955) equation

Further studies by Kohler *et al.* (1955) showed that considering the nonlinear relationship between VPD and pan-evaporation in the studied data leads to more precise calculations. The new equation, known as the Kohler–Nordonson–Fox equation

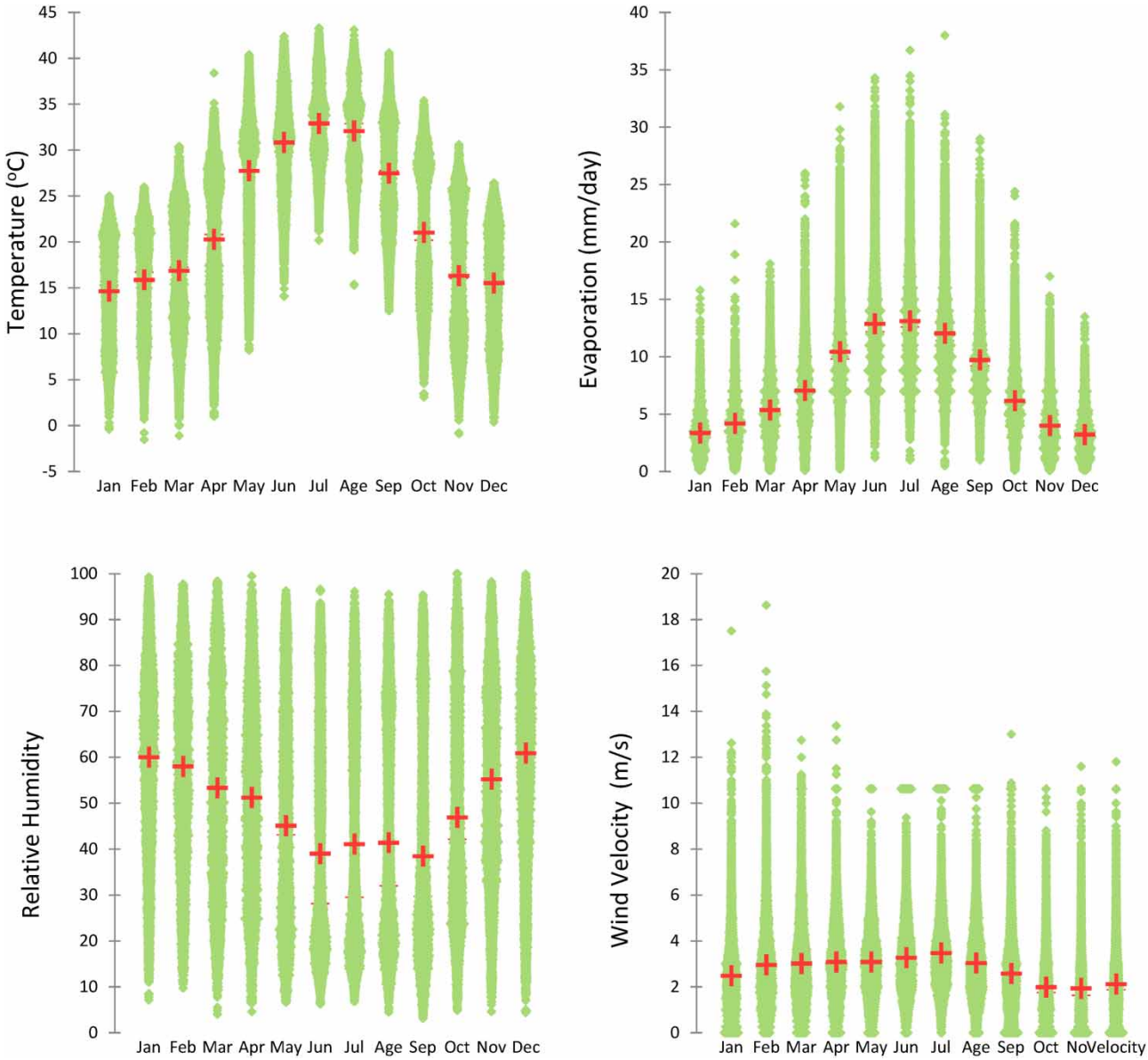

Figure 3 | Scattergrams of climatic components in arid and semi-arid regions.

(Izady *et al.* 2020), is considered a development of the Kohler (1954) equation (Althoff *et al.* 2020).

$$E = (e_s - e_d)^{\beta_{12}} (\beta_{13} + \beta_{14} V_P)$$

In this equation, E is the calculated pan-evaporation (inches per day); $(e_s - e_d)$ is the VPD (inches of mercury); and V_P is the wind velocity at the height of the installation of the evaporation pan from the ground (miles per day). The $\beta_{12} = 0.88$, $\beta_{13} = 0.37$, $\beta_{14} = 0.0041$ are the coefficients of the K–N–F (1955) equation.

2.4.5. Linacre (1994) equation

The equation presented by Linacre (1994) can be considered an improvement on the Linacre (1977) equation (Stephens *et al.* 2018). The new equation (wind velocity) was also added to the mathematical form of the equation as a practical input to

evaporation, which uses five coefficients to calculate evaporation.

$$E = \frac{[\beta_{15}\, T - \beta_{16} + \beta_{17}\, V\,(T - T_d)]}{\left[\beta_{18} + \frac{\beta_{19}}{S}\right]}$$

Considering the equation, E is th calculated pan-evaporation (mm/day); V_P is the wind velocity at the height of 2 m above the ground (m/s), T is the average daily air temperature (°C), T_d is the dew point temperature (°C); and $\beta_{15} = 21$, $\beta_{16} = 166$, $\beta_{17} = 6$, $\beta_{18} = 28$, $\beta_{19} = 46$ are the coefficients of Linacre (1994) equation. Also, S is the slope of the psychrometric curve in millibars of mercury obtained from the following equation (Murray 1967; Basnyat 1987):

$$S = e_s \left(\frac{4098.03}{(T + 237.3)^2}\right)$$

In the above equation, T is the average daily temperature (°C) and e_s is the saturated vapor pressure at the water surface, which can be obtained from the following relation (Xu & Singh 2002):

$$e_s = 6.1078 \exp\left[\frac{17.2694\, T}{(T + 237.3)}\right]$$

2.4.6. Papadakis (1961) equation

In this equation, Papadakis (1961) presented a simple linear relationship between the VPD, and evaporation is applied (Basnyat 1987). This equation uses only one coefficient to calculate evaporation using climatic components temperature and relative humidity (Bozorgi *et al.* 2020).

$$E = \beta_{20}(e_s - e_d)$$

E is the calculated pan-evaporation (mm/day); $(e_s - e_d)$ is the VPD (mbar), and finally $\beta_{20} = 0.5626$ is the coefficient of the Papadakis (1961) equation.

2.4.7. Kohler (1954) equation

This equation was developed by Kohler (1954). Also known as the Hefner equation, the Kohler (1954) equation can be considered an extended mathematical form of the Papadakis (1961) equation, in which the wind velocity component is added to the mathematical form of the equation to improve the evaporation calculation (Song *et al.* 2020).

$$E = (e_s - e_d)(\beta_{21} + \beta_{22}\, V_P)$$

E is the calculated pan-evaporation (inches per day); $(e_s - e_d)$ is the VPD (inches of mercury); V_P is the wind velocity at the standard height of the evaporation pan installed from the ground (miles per day); and $\beta_{21} = 0.42$, $\beta_{22} = 0.004$ are the coefficients of the Kohler (1954) equation.

2.5. The process of improving empirical mathematical equations

It is necessary to use the data from these regions to improve the precision of the empirical mathematical equations in calculating the pan-evaporation in arid and semi-arid regions. In the improvement process, using an optimization algorithm can significantly impact better equation precision. In this research, the Nelder–Mead (N–M) algorithm embedded in the MATLAB environment has been used. A simplex comprises $n + 1$ vertices in an n-dimensional space, each representing a potential solution to the optimization problem. In every iteration, the worst solution is replaced by a better solution obtained by performing some operations on the vertices (Kshirsagar *et al.* 2020). The procedure implemented for applying the N–M algorithm is illustrated in Figure 4.

2.6. Precision of modeling

It is necessary to use indicators that consider the precision of modeling to assess the precision of equations (Ansarifar *et al.* 2020). Many indicators have been devised to assess the precision of equations. However, the indicators should be chosen

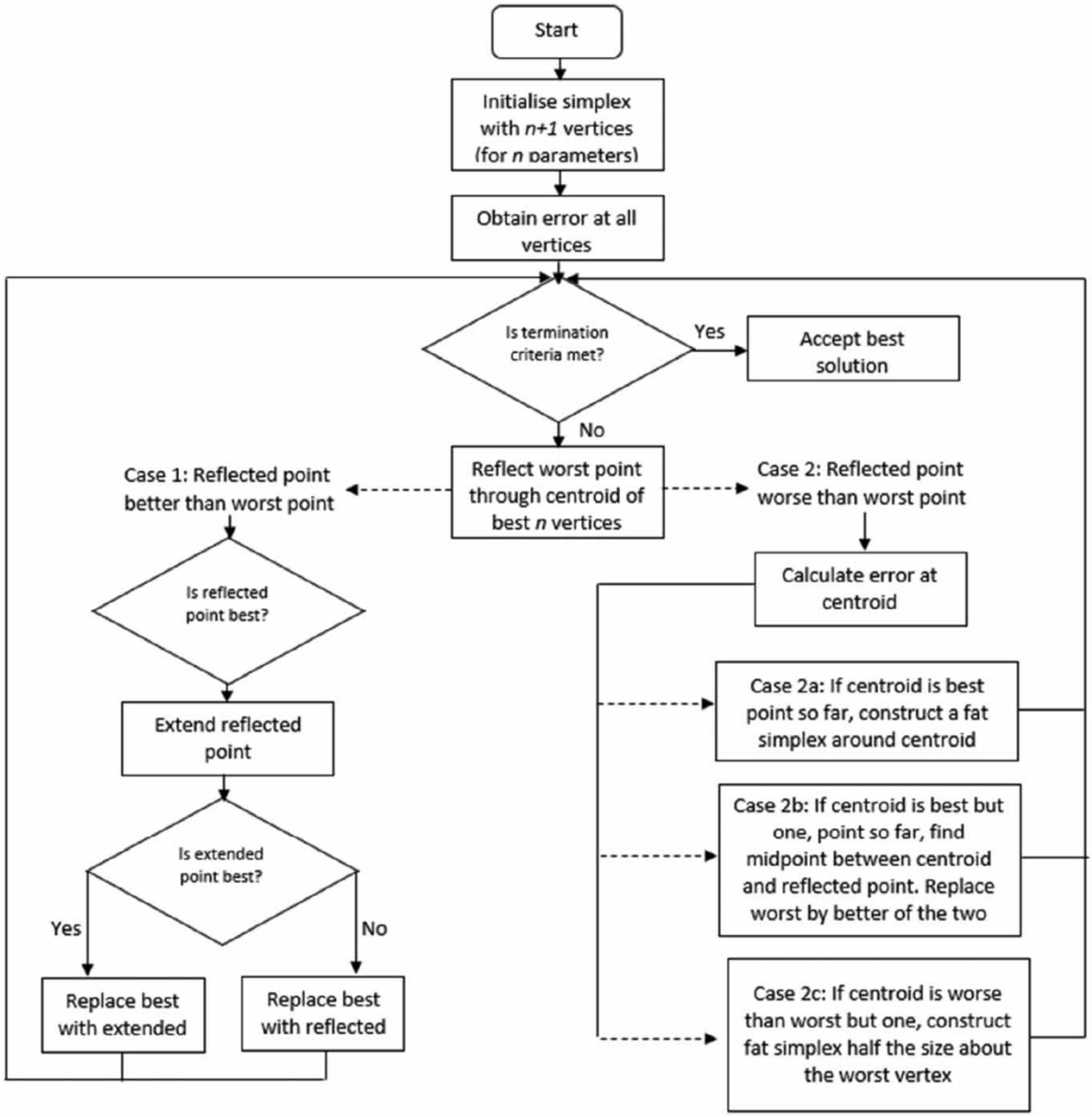

Figure 4 | The flowchart of the N–M algorithm (Kshirsagar *et al.* 2020).

based on the equations' properties. In this study, two indicators, mean bias error (MBE) and normalized root mean square error (nRMSE), were used to assess the precision of the equations. The first indicator indicates overestimated and underestimated patterns of evaporation equations (Rincón *et al.* 2018). The second indicator shows the precision of the equations in calculating evaporation (Norouzi *et al.* 2021). The mathematical form of these indicators is shown in the lower part of the presentation.

$$\mathrm{MBE} = \frac{1}{n}\sum_{i=1}^{n}(p_i - o_i) \times 100$$

$$\mathrm{nRMSE} = \frac{\sqrt{\frac{1}{n}\sum_{i=1}^{n}(p_i - o_i)^2}}{\bar{o}} \times 100$$

In the presented equations, p_i and o_i are used for the calculated and recorded values. If the modeling is exact, both indicators will have a zero value. Suppose the number of equations under study is high and more than one indicator is used to assess modeling precision. In that case, another indicator is needed to overcome the analysis challenges. This research uses the compound performance indicator (CPI) as a compound indicator (Despotovic *et al.* 2015). The CPI indicator converts the values of the nRMSE and MBE indicators into an indicator, facilitating the analysis of the results. In this method, first, the values of the two main indicators are scaled, which prevents the adverse impact of different values and ranges of the two main indicators on the CPI indicator. The following equation scales the main indicators (Manju & Sandeep 2019):

$$z_{\text{scaled}} = \left(\frac{z - z_{\min}}{z_{\max} - z_{\min}} \right)$$

where $z_{\min}$, $z_{\max}$, z_{scaled}, and z are the minimum, maximum, scaled, and natural values of the indicator. Consequently, the maximum and minimum scaled indicators will be 1 and 0. The mathematical form of the mentioned equation indicates the values of two main indicators ranging from 0 to 1. The following equation calculates the compound indicator (Manju & Mavi 2021:.

$$\text{CPI} = \sum_{k=1}^{2} b_k (f_k - h_{lk})$$

The b_k is considered 1 for nRMSE and MBE. The f_k is equal to the median of scaled values of precision indicator k. Moreover, h_{lk} is used for scaled values of indicator l for equation k. To the mathematical form of CPI, it is clear that the higher the value of this indicator, the higher the precision of the studied empirical mathematical equations for pan-evaporation and vice versa (Feng *et al.* 2018).

3. RESULTS

3.1. Improvement results

The empirical mathematical equations for pan-evaporation calculation were improved using the N–M algorithm. Changes in the values of the objective functions of the empirical mathematical equations for calculating pan-evaporation are presented in Figure 5. In these plots, the horizontal and vertical axes represent the iterations and values of the objective functions, respectively. Table 3 shows the values of the equation coefficients for pan-evaporation before and after improvement. Paying close attention to how the coefficients of the equations change before and after the improvement yields remarkable results. The coefficient changed only 12% after improvement for the Papadakis (1961) equation. This low change is very important, considering that this empirical mathematical equation has only one coefficient. In the two equations of Linacre (1994) and Linacre (1977), the values of the two coefficients changed from 166 and 15 to 0. In the Linacre (1977) equation, improvement made the mathematical form of the equation simpler. This finding means that the original mathematical form of the Linacre (1977) equation is not suitable enough to calculate pan-evaporation in arid and semi-arid regions.

3.2. Spatial distribution of equation precision indicators

Values of nRMSE and MBE indicators were calculated considering the 14 equations used in this study (7 original and 7 improved empirical mathematical equations). This study used a map to show the spatial precision of equations. Spatial distributions of the indicators for the original and improved equations are illustrated in Figures 6 and 7. Figure 8 used plots to visualize the equations' precision and the overestimated and underestimated pattern errors. There is no access to data to improve the equations in many regions, so assessing the original equations is essential. According to this fact, the comparative assessment of the original equations and the comparative assessment of the original and improved empirical mathematical equations were presented together.

3.3. Assessment of the original empirical mathematical equations to calculate pan-evaporation

The indicators for the precision of empirical mathematical equations to calculate pan-evaporation are presented in Figures 6–8. In addition, the CPI indicator of the original equations is shown in Figure 9. Among the original empirical mathematical equations, the three equations K–N–F (1955), Kohler (1954), and Papadakis (1961) had more precise answers in calculating the pan-evaporation than the other equations. These relevant results attract attention considering the simple mathematical

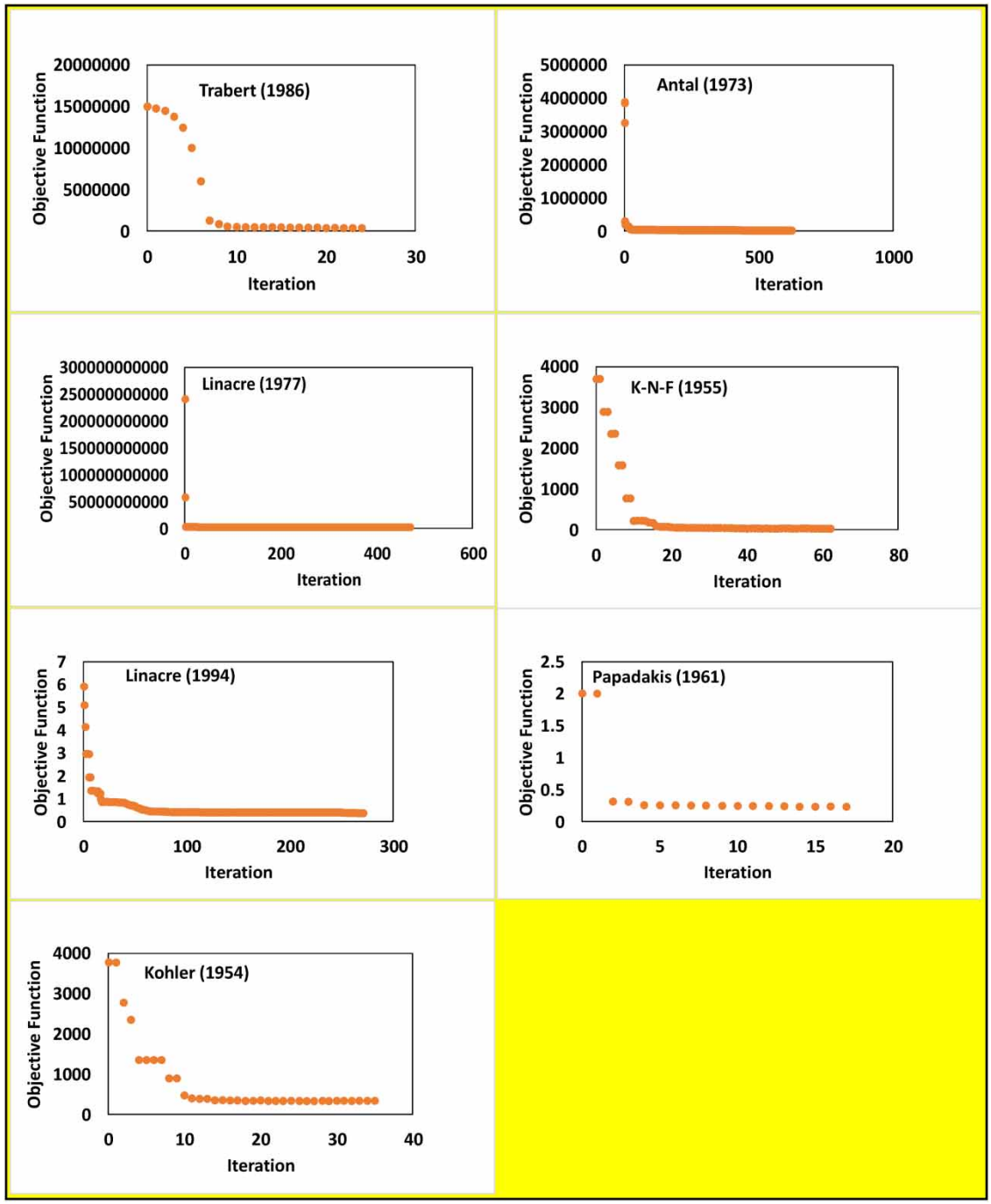

Figure 5 | Changes in the objective function in the improvement process for the pan-evaporative empirical mathematical equations.

form of these equations, especially the Papadakis equation (1961). Comparing the original equations reveals that Trabert (1896) and Linacre (1977) equations had the least precise calculations. Applying original coefficients extracted in other regions is one reason for unsuitable results. Comparing the results of equations in the overestimated or underestimated pattern field is very important (Béchet *et al.* 2018). Assessment of the original equations shows that the equations of Antal (1973), Papadakis (1961), and Linacre (1994) tend to overestimate, while the Kohler (1954), K–N–F (1955), Linacre (1977), and Trabert (1896) equations tend to underestimate. The Antal (1973) equation had the most overestimated, and the Trabert equation (1896) had the most underestimated pattern in the calculations. The K–N–F (1955) equation shows the lowest

Table 3 | Original and improved values of empirical mathematical equation coefficients in arid and semi-arid regions

Empirical mathematical equation	Coefficients	Default value	Improved value	Changes in percent
Trabert (1896)	β_1	0.3075	2.8374	2.5
Antal (1973)	β_2	1.1	0.6	−0.5
	β_3	0.7	0.6	−0.1
	β_4	1	1.1	0.1
	β_5	273	2.4	−270.6
	β_6	4.8	0.5	−4.3
Linacre (1977)	β_7	700	1,009.6	309.6
	β_8	0.006	0.008	0.002
	β_9	100	139	39
	β_{10}	15	0	−15
	β_{11}	80	59	−21
K–N–F (1955)	β_{12}	0.88	0.7	−0.18
	β_{13}	0.37	0.58	0.21
	β_{14}	0.0041	0.0015	−0.0026
Linacre (1994)	β_{15}	21	21.3	0.3
	β_{16}	166	0	−166
	β_{17}	6	4	−2
	β_{18}	28	60	32
	β_{19}	46	28	−18
Papadakis (1961)	β_{20}	0.563	0.5	−0.1
Kohler (1954)	β_{21}	0.42	0.65	−0.23
	β_{22}	0.004	0.001	−0.003

overestimated/underestimated pattern compared to other equations, which indicates a suitable equilibrium in the pan-evaporation calculations with this equation.

3.4. Assessment of original and improved equations

Precision indicators are presented in Figures 6–8, and values of CPI indicators are illustrated in Figure 10. The number of equations after improvement increased from 7 to 14, with 7 being the original equation and 7 being the improved equation. The improved K–N–F (1955) equation was the best among the 14 equations studied. Then the improved Linacre (1994) equation can be considered the second most suitable equation. The most important disadvantage of this equation is that it did not lead to suitable results in the southern regions. In contrast, in other regions, the precision of this equation was suitable. The similarity between the two improved K–N–F (1955) and improved Linacre (1994) is that wind velocity is considered an input component. Assessment of the 14 equations studied reveals that the original Trabert (1896) and Linacre (1977) equations led to the most unsuitable results regarding computational precision. In addition to the unsuitable original coefficients of these equations, the unsuitable mathematical form has also been effective in these unsuitable results. Among these 14 equations, the lowest value of overestimated/underestimated pattern is improved Papadakis (1961), an important result in related studies. After the improved Papadakis (1961), the improved Kohler (1954) and the original K–N–F (1955) equations had limited underestimated/overestimated behavior. Among these 14 equations, the original Trabert (1896) and Linacre (1977) equations had the largest overestimated/underestimated values, which confirmed the unsuitable results of these equations.

3.5. Impact of improvement on original empirical mathematical equations to calculate pan-evaporation

A comparative study of the original and improved equations reveals that most improvements occurred in the Trabert equation. It is crucial because the improved Trabert (1896) equation indicates its unsuitable precision compared to other

Figure 6 | Spatial distribution of MBE indicators in arid and semi-arid regions.

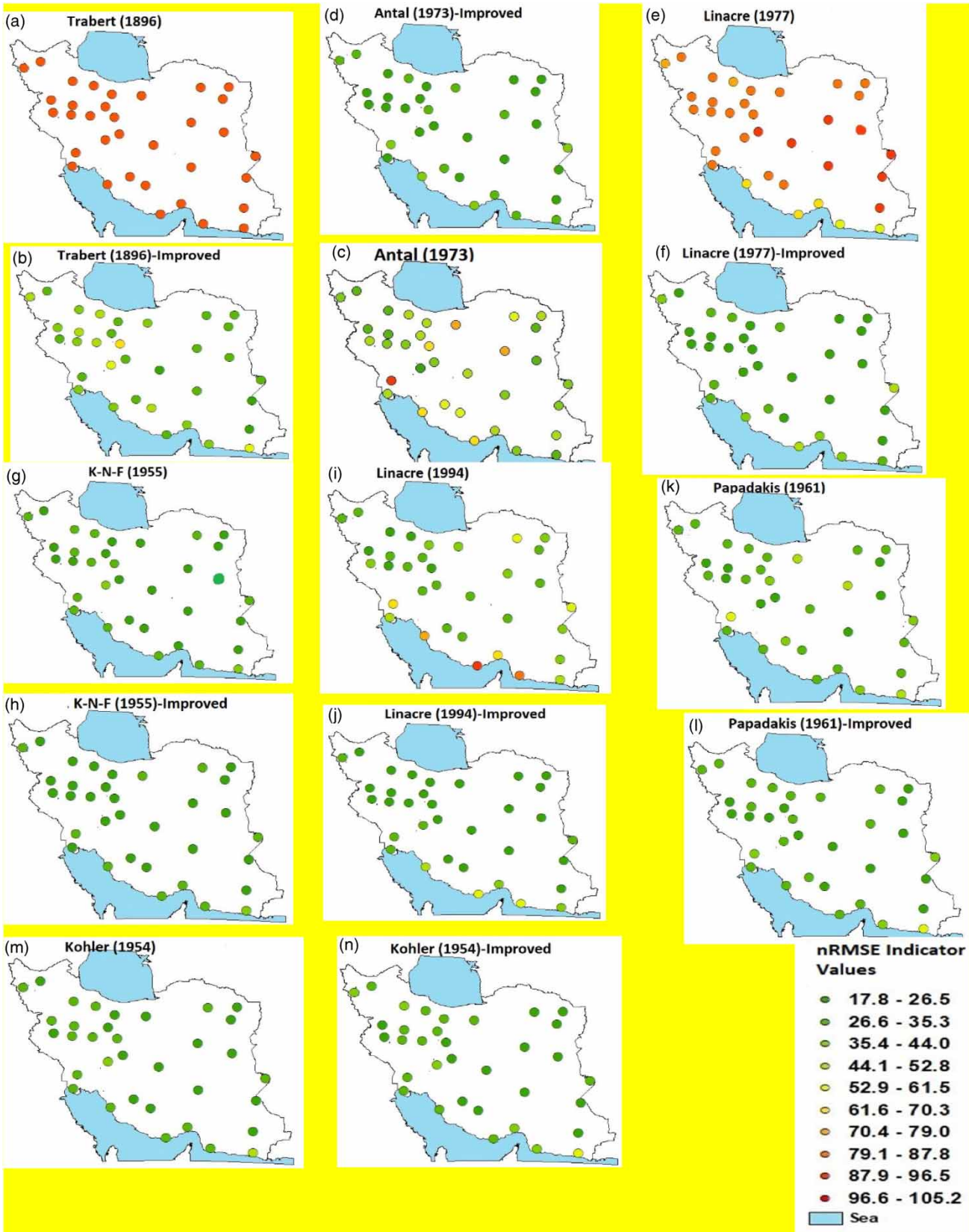

Figure 7 | Spatial distribution of nRMSE indicator in arid and semi-arid regions.

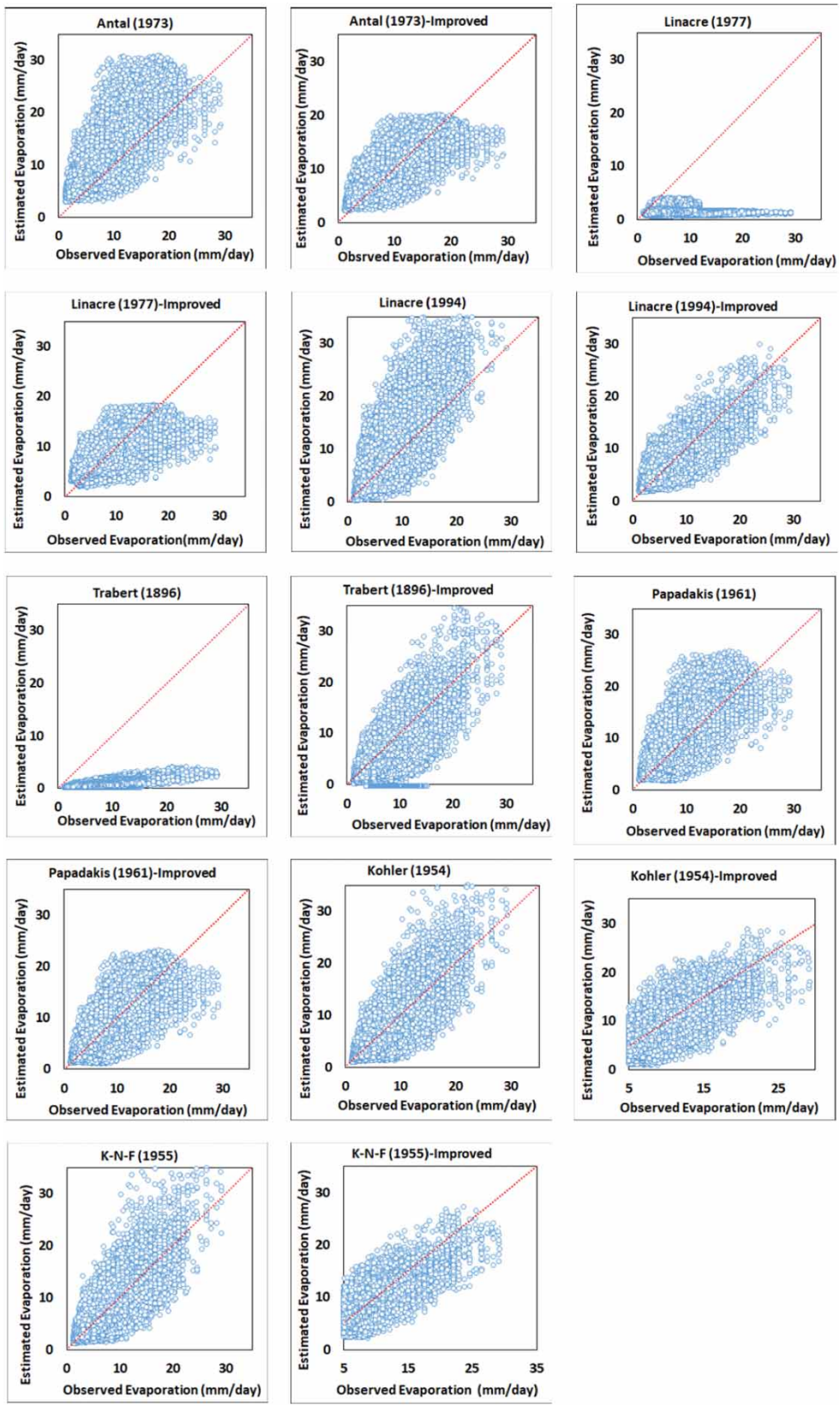

Figure 8 | Visual assessment of the precision of empirical mathematical pan-evaporation equations in arid and semi-arid regions.

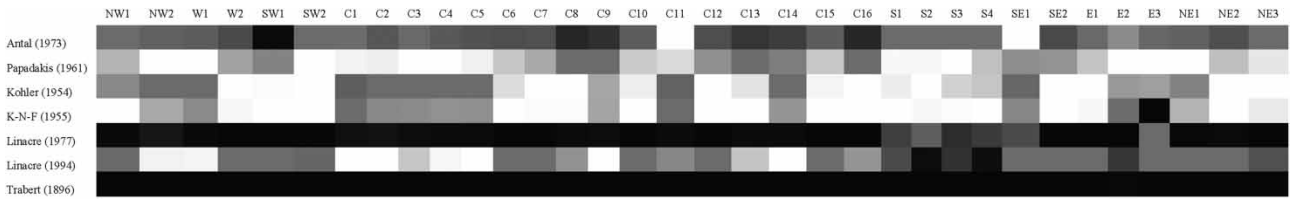

Figure 9 | The CPI indicator for original pan-evaporation empirical mathematical equations in arid and semi-arid regions.

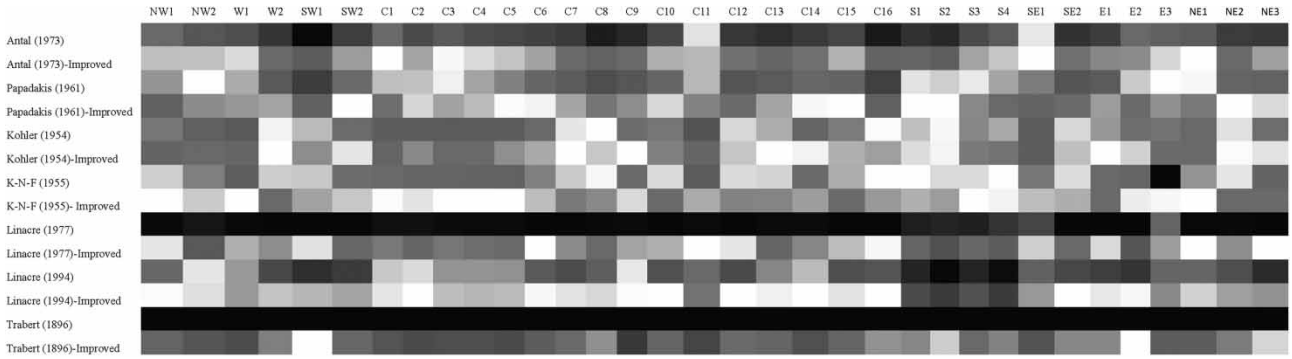

Figure 10 | The CPI indicator original and improved pan-evaporation empirical mathematical equations in arid and semi-arid regions.

equations. Comparing the precision of the original and improved Kohler (1954), Papadakis (1961), and K–N–F (1955) equations reveals that compared to other equations, the improvement had the least impact on them. Another critical point is that the precision of these equations has been suitable in both original and improved cases, and this shows that these equations can be considered to have consistency in arid and semi-arid regions. The original and improved K–N–F (1955) among all equations led to greater precision in calculating the pan-evaporation. After improving, the overestimated pattern of the Antal (1973) and Linacre (1994) equations, as well as the underestimated pattern of the Kohler (1954), Trabert (1896), and Linacre (1977) equations has decreased. The original equation of Papadakis (1961) was slightly more than estimated, while the improved equation had a limited estimate of limited behavior. However, in general, the pattern of this equation became more balanced after improvement. The original K–N–F (1955) equation has a somewhat underestimated problem; the improved equation is finely overestimated after improvement.

3.6. Spatial assessment

Attention to the impact of spatial variations (Figures 6 and 7) on the results of the studied equations has led to the revelation of specific results. On the one hand, the nRMSE indicator shows the highest precision in the eastern and northwestern regions and the lowest precision in the southern and southeastern regions. On the other hand, if the overestimated/underestimated pattern is considered the basis for the decision, the best results can be seen in the western and northeastern regions and the lowest precision in the southern and southwestern regions. In general, the precision of the equations in the southern regions has been less than in other regions. This pattern is generally recognizable in the south, southeast, and southwest. Also, in the western, northeastern, eastern, and northwestern regions, the precision of the equations in calculating the pan-evaporation is higher than in other regions. In the central regions, the precision of the equations is in the median situation compared to other regions.

4. DISCUSSION

Considering Figure 5, in which changes in the objective function are plotted for consecutive iterations, it is clear that the N–M optimization algorithm has a suitable performance to calculate the coefficients of the studied equations. Similar results of the suitability of this algorithm in improving the equations applied in the field of water and environment have been reported (Liu *et al.* 2015). There is a coefficient in the mathematical form of Papadakis (1961) and Trabert (1896) equations. Considering the difference between the coefficients of these equations, before and after improvement shows the apparent difference

between the two equations in the precision of calculating pan-evaporation in arid and semi-arid regions. After improving, the coefficient of the Trabert equation (1896) has changed a lot. However, the coefficient has changed slightly in the Papadakis equation (1961). This result indicates that the original equation of Trabert (1896) is an unsuitable equation, and the original Papadakis (1961) equation is suitable for calculating pan-evaporation in arid and semi-arid regions. The variations between the original and improved coefficients depend on the reported original values and a function of the mathematical form of the equations. Suppose the mathematical form of these two equations is similar in terms of the precision of pan-evaporation calculation in arid and semi-arid regions. In that case, the precision of the results should be relatively similar after improvement, but such a result was not obtained. It means that the mathematical form of the Trabert (1896) equation is not precise enough to calculate pan-evaporation in arid and semi-arid regions.

Among the original equations and according to all recorded data series studied, the highest precision in calculating pan-evaporation was obtained by using the K–N–F (1955) equation and then Kohler (1954) and Papadakis (1961) equations. The K–N–F (1955) equation was the best original in arid and semi-arid regions. In the mathematical form of this equation, there are two distinct and essential features. One considers wind velocity, and the other is the nonlinear relationship between VPD and pan-evaporation. Improving precision concerning the use of nonlinear relationships in evaporation-related studies has been emphasized by Liu *et al.* (2018), and the findings of this study confirm the mentioned research. The main difference between this equation and the Kohler (1954) equation is the existence of this relation in a nonlinear mathematical form. On the other hand, this finding emphasizes the effective role of wind in arid and semi-arid regions in evaporation. Based on the above, the suitable mathematical form of the K–N–F (1955) equation can be considered a dominant factor in achieving the suitable precision of calculations.

As seen in the mathematical form of the equations, Papadakis (1961) has the simplest mathematical form of the studied equations. This equation's suitable results confirm Bozorgi *et al.*'s research results (2021). The Papadakis (1961) equation was developed based on temperature and relative humidity, and the K–N–F (1955) and Kohler (1954) equations, besides these climatic components, also use wind velocity. According to the mathematical form of these equations and the relatively close precision of the results, it can be found that in arid and semi-arid regions, the most critical component affecting evaporation is the relative humidity and temperature pan. Then wind velocity is the third effective component. The significant impact of relative humidity and temperature on evaporation has also been considered in Burn & Hesch (2007) study.

Among the 14 original and improved equations in this study, the improved K–N–F (1955) and Linacre (1994) equations had the highest precision in calculating the pan-evaporation. In the improved K–N–F (1955) equation, wind velocity is included in the calculations as a component alongside temperature and relative humidity. In the Linacre (1994) equation, although the wind velocity component is used, the relative humidity component is not used. Notably, the weakness of the Linacre (1994) equation has been in the recorded data series in the southern regions. An important feature of these regions is the high relative humidity. In addition to the above, it can be concluded that the application of the Linacre (1994) equation has been improved. Although it has had good results in regions of high relative humidity, the precision of this equation is significantly reduced. While in these conditions, the empirical mathematical equations that use the relative humidity component have led to more precise calculations.

The least precise results in the calculations were due to the use of the Trabert (1896) and Linacre (1977) equations. The first reason for these unsuitable results is related to the original coefficients of these equations because the precision of these two equations has increased after improving. Although the precision of these two equations has improved in the improved process, they still do not have high precision compared to other equations. Therefore, it can be concluded that the main limitation of these two equations goes back to their mathematical form. In the Trabert (1896) equation, the relationship between wind velocity and evaporation is assumed to be radical. This mathematical form of applying wind velocity means that, despite the inclusion of temperature and relative humidity components, this equation does not have the acceptable ability to calculate pan-evaporation in arid and semi-arid regions. It seems that in the Linacre (1977) equation, components such as latitude and elevation cause the inability of this equation to calculate pan-evaporation with acceptable precision. In addition, this equation does not use wind velocity and relative humidity to calculate evaporation. At the same time, the findings of this study indicate the significant impact of these two components on the precision of calculating pan-evaporation in arid and semi-arid regions. According to the findings, the limitation in the mathematical form of these two equations for calculating pan-evaporation in arid and semi-arid regions becomes more apparent. Generally, the precision of pan-evaporation calculation by the set of equations in the southern regions has been less than in other regions. These regions are characterized by high relative humidity and temperature compared to other regions.

Further attention shows that the cause of this problem is the mathematical form of equations that do not use relative humidity. In other words, this group of equations has reduced the precision in assessing the set of equations together. Also, the precision of the equations in the western and eastern regions has been better than in other regions. The most crucial difference between these regions and the southern region is the relative humidity and temperature. These findings emphasize the impact of spatial distribution on the precision of the equations, consistent with the findings of Feng *et al.* (2018).

5. CONCLUSION

Evaporation is extremely important in an arid and semi-arid region that faces water shortages. The most well-known method of recording evaporation data is to use an evaporation pan. In many regions, pan-evaporation data are unavailable, so empirical mathematical equations are used as a practical alternative. Applying empirical mathematical equations in different climatic conditions can produce a wide range of results. It is usually fragile in arid and semi-arid regions due to water shortages, agriculture, environment, and socio-economic conditions. In such cases, there is more need for suitable and precise calculations of pan-evaporation. In arid and semi-arid regions, relative humidity is generally low, the temperature is high, and as a result, the application of empirical mathematical equations that are not only developed in these regions can be of unsuitable precision. This research studied the precision of the seven original empirical mathematical equations and the improved equations to assess the pan-evaporation equations focusing on arid and semi-arid regions. A review of the results of this study shows that the K–N–F (1955), Kohler (1954), and Papadakis (1961) equations had the highest precision among the original equations. It shows the significant impact of three components of temperature, relative humidity, and wind velocity in arid and semi-arid regions on the amount of pan-evaporation. Among the 14 studied equations, the best precision belongs to the improved K–N–F (1955), Linacre (1994), and Kohler (1954) equations. However, the equations that rank next are also improved from the original ones, indicating the need to improve the equations in arid and semi-arid regions.

DATA AVAILABILITY STATEMENT

Data cannot be made publicly available; readers should contact the corresponding author for details.

CONFLICT OF INTEREST

The authors declare there is no conflict.

REFERENCES

Adnan, R. M., Malik, A., Kumar, A., Parmar, K. S. & Kisi, O. 2019 Pan evaporation modeling by three different neuro-fuzzy intelligent systems using climatic inputs. *Arabian Journal of Geosciences* **12** (19), 1–14.

Alekseev, A. O., Mitenko, G. V. & Sharyi, P. A. 2020 Quantitative estimates of paleoenvironmental changes in the late holocene in the south of the east European plain as recorded in the magnetic properties of soils. *Eurasian Soil Science* **53** (12), 1677–1686.

Alsumaiei, A. A. 2020 Utility of artificial neural networks in modeling pan evaporation in hyper-arid climates. *Water* **12** (5), 1508.

Althoff, D., Rodrigues, L. N. & da Silva, D. D. 2020 Impacts of climate change on the evaporation and availability of water in small reservoirs in the Brazilian savannah. *Climatic Change* **159** (2), 215–232.

American Meteorological Society 2006 *Glossary of Meteorology*. Available from: http://amsglossary.allen press .com/glossary

Ansarifar, M. M., Salarijazi, M., Ghorbani, K. & Kaboli, A. R. 2020 Spatial estimation of aquifer's hydraulic parameters by a combination of borehole data and inverse solution. *Bulletin of Engineering Geology and the Environment* **79** (2), 729–738.

Antal, E. 1973 Evapotranspiration from com field. Term paper submitted for Dr. R. F. Dale's Agronomy 537 class. Received from personal communication with Dr. Dale (Dept. of Agronomy, Purdue University, Indiana).

Basnyat, M. B. 1987 *Estimation of Daily Class A Pan Evaporation from Meteorological Data*. Doctoral Dissertation, Iowa State University.

Béchet, Q., Sialve, B., Steyer, J. P., Shilton, A. & Guieysse, B. 2018 Comparative assessment of evaporation models in algal ponds. *Algal Research* **35**, 283–291.

Bozorgi, A., Bozorg-Haddad, O., Sima, S. & Loáiciga, H. A. 2020 Comparison of methods to calculate evaporation from reservoirs. *International Journal of River Basin Management* **18** (1), 1–12.

Bozorgi, A., Bozorg-Haddad, O., Sima, S. & Loáiciga, H. A. 2021 Comparison of methods for estimating loss from water storage by evaporation and impacts on reservoir management. *Water and Environment Journal* **35** (1), 218–228.

Burn, D. H. & Hesch, N. M. 2007 Trends in evaporation for the Canadian Prairies. *Journal of Hydrology* **336** (1–2), 61–73.

Chaudhari, N., Londhe, S. & Khare, K. 2012 Estimation of pan evaporation using soft computing tools. *International Journal of Hydrology Science and Technology* **2** (4), 373–390.

Chen, J. L., Yang, H., Lv, M. Q., Xiao, Z. L. & Wu, S. J. 2019 Estimation of monthly pan evaporation using support vector machine in three Gorges Reservoir Area, China. *Theoretical and Applied Climatology* **138** (1), 1095–1107.

Costa, A. C. & Soares, A. 2012 Local spatiotemporal dynamics of a simple aridity index in a region susceptible to desertification. *Journal of Arid Environments* **87**, 8–18.

Croitoru, A. E., Piticar, A., Imbroane, A. M. & Burada, D. C. 2013 Spatiotemporal distribution of aridity indices based on temperature and precipitation in the extra-Carpathian regions of Romania. *Theoretical and Applied Climatology* **112** (3), 597–607.

Dehghanipour, M. H., Karami, H., Ghazvinian, H., Kalantari, Z. & Dehghanipour, A. H. 2021 Two comprehensive and practical methods for simulating pan evaporation under different climatic conditions in Iran. *Water* **13** (20), 2814.

Deniz, A., Toros, H. & Incecik, S. 2011 Spatial variations of climate indices in Turkey. *International Journal of Climatology* **31** (3), 394–403.

Despotovic, M., Nedic, V., Despotovic, D. & Cvetanovic, S. 2015 Review and statistical analysis of different global solar radiation sunshine models. *Renewable and Sustainable Energy Reviews* **52**, 1869–1880.

Dlouhá, D., Dubovský, V. & Pospíšil, L. 2021 Optimal calibration of evaporation models against Penman–Monteith equation. *Water* **13** (11), 1484.

Feng, Y., Jia, Y., Zhang, Q., Gong, D. & Cui, N. 2018 National-scale assessment of pan evaporation models across different climatic zones of China. *Journal of Hydrology* **564**, 314–328.

Flammini, A., Corradini, C., Morbidelli, R., Saltalippi, C., Picciafuoco, T. & Giráldez, J. V. 2018 Experimental analyses of the evaporation dynamics in bare soils under natural conditions. *Water Resources Management* **32** (3), 1153–1166.

Ghumman, A. R., Ghazaw, Y. M., Alodah, A., Shafiquzzaman, M. & Haider, H. 2020 Identification of parameters of evaporation equations using an optimization technique based on pan evaporation. *Water* **12** (1), 228.

Guan, Y., Mohammadi, B., Pham, Q. B., Adarsh, S., Balkhair, K. S., Rahman, K. U., Nguyen, T. T. L. & Tri, D. Q. 2020 A novel approach for predicting daily pan evaporation in the coastal regions of Iran using support vector regression coupled with krill herd algorithm model. *Theoretical and Applied Climatology* **142** (1), 349–367.

Izady, A., Nikoo, M. R., Bakhtiari, P. H., Baawain, M. S., Al-Mamari, H., Msagati, T. A., Nkambule, T. T., Al-Maktoumi, A., Chen, M. & Prigent, S. 2020 Risk-based stochastic optimization of evaporation ponds as a cost-effective and environmentally-friendly solution for the disposal of oil-produced water. *Journal of Water Process Engineering* **38**, 101607.

Jones, F. E. 2018 *Evaporation of Water: With Emphasis on Applications and Measurements*. CRC Press, Boca Raton.

Kohler, M. A. 1954 *Lake and Pan Evaporation*. Water-Loss Investigations: Lake Hefner Studies, Technical Report, United States Geological Survey Professional Paper, 269, 127–149.

Kohler, M. A., Nordenson, T. J. & Fox, W. E. 1955 *Evaporation from Pans and Lakes*, Vol. 30. US Government Printing Office, Washington, DC.

Kshirsagar, R., Jones, S., Lawrence, J. & Tabor, J. 2020 Optimization of TIG welding parameters using a hybrid Nelder Mead-evolutionary algorithms method. *Journal of Manufacturing and Materials Processing* **4** (1), 10.

Kumar, M., Kumari, A., Kumar, D., Al-Ansari, N., Ali, R., Kumar, R., Kumar, A., Elbeltagi, A. & Kuriqi, A. 2021 The superiority of data-driven techniques for estimation of daily pan evaporation. *Atmosphere* **12** (6), 701.

Linacre, E. T. 1977 A simple formula for estimating evaporation rates in various climates, using temperature data alone. *Agricultural Meteorology* **18** (6), 409–424.

Linacre, E. T. 1994 Estimating US Class A pan evaporation from few climate data. *Water International* **19** (1), 5–14.

Liu, X., Tu, Q., Hua, Z., Huang, W., Xing, L. & Zhou, Y. 2015 Multi-parameter identification of a two-dimensional water-quality model based on the Nelder–Mead simplex algorithm. *Hydrology Research* **46** (5), 711–720.

Liu, X., Liu, C. & Brutsaert, W. 2018 Investigation of a generalized nonlinear form of the complementary principle for evaporation estimation. *Journal of Geophysical Research: Atmospheres* **123** (8), 3933–3942.

Lu, X., Ju, Y., Wu, L., Fan, J., Zhang, F. & Li, Z. 2018 Daily pan evaporation modeling from local and cross-station data using three tree-based machine learning models. *Journal of Hydrology* **566**, 668–684.

Majhi, B., Naidu, D., Mishra, A. P. & Satapathy, S. C. 2020 Improved prediction of daily pan evaporation using deep-LSTM model. *Neural Computing and Applications* **32** (12), 7823–7838.

Majidi, M., Alizadeh, A., Farid, A. & Vazifedoust, M. 2015 Estimating evaporation from lakes and reservoirs under limited data condition in a semi-arid region. *Water Resources Management* **29** (10), 3711–3733.

Manju, S. & Mavi, S. 2021 Harmonic analysis of annual global irradiation in the cities of India. *Journal of Cleaner Production* **295**, 126461.

Manju, S. & Sandeep, M. 2019 Prediction and performance assessment of global solar radiation in Indian cities: A comparison of satellite and surface measured data. *Journal of Cleaner Production* **230**, 116–128.

McMahon, T. A., Peel, M. C., Lowe, L., Srikanthan, R. & McVicar, T. R. 2013 Estimating actual, potential, reference crop and pan evaporation using standard meteorological data: A pragmatic synthesis. *Hydrology and Earth System Sciences* **17** (4), 1331–1363.

McMahon, T. A., Finlayson, B. L. & Peel, M. C. 2016 Historical developments of models for estimating evaporation using standard meteorological data. *Water* **3** (6), 788–818.

Modabber-Azizi, S., Salarijazi, M. & Ghorbani, K. 2023 A novel approach to recognize the long-term spatial-temporal pattern of dry and wet years over Iran. *Physics and Chemistry of the Earth, Parts A/B/C* **131**, 103426.

Mohammadi, M., Salarijazi, M., Ghorbani, K. & Dehghani, A. A. 2023 Coastal cities-wide estimation of daily class A pan evaporation from few hydrometeorological variables. *Urban Water Journal* **20** (7), 782–800.

Murray, F. W. 1967 On the computation of saturated vapor pressure. *Journal of Applied Meteorology* **6**, 203–204.
Norouzi, R., Sihag, P., Daneshfaraz, R., Abraham, J. & Hasannia, V. 2021 Predicting relative energy dissipation for vertical drops equipped with a horizontal screen using soft computing techniques. *Water Supply* **21** (8), 4493–4513.
Nyamtseren, M., Feng, Q. & Deo, R. 2018 A comparative study of temperature and precipitation-based aridity indices and their trends in Mongolia. *International Journal of Environmental Research* **12** (6), 887–899.
Papadakis, J. 1961 *Climatic Tables for the World*. Published by the author, Buenos Aires.
Patle, G. T., Chettri, M. & Jhajharia, D. 2020 Monthly pan evaporation modelling using multiple linear regression and artificial neural network techniques. *Water Supply* **20** (3), 800–808.
Pellicone, G., Caloiero, T. & Guagliardi, I. 2019 The De Martonne aridity index in Calabria (Southern Italy). *Journal of Maps* **15** (2), 788–796.
Rincón, A., Jorba, O., Frutos, M., Alvarez, L., Barrios, F. P. & González, J. A. 2018 Bias correction of global irradiance modelled with weather and research forecasting model over Paraguay. *Solar Energy* **170**, 201–211.
Salarijazi, M., Ghorbani, K., Mohammadi, M., Ahmadianfar, I., Mohammadrezapour, O., Naser, M. H. & Yaseen, Z. M. 2023 Spatial-temporal estimation of maximum temperature high returns periods for annual time series considering stationary/nonstationary approaches for Iran urban area. *Urban Climate* **49**, 101504.
Sebbar, A., Heddam, S. & Djemili, L. 2019 Predicting daily pan evaporation (E pan) from dam reservoirs in the Mediterranean Regions of Algeria: OPELM vs OSELM. *Environmental Processes* **6** (1), 309–319.
Seifi, A. & Soroush, F. 2020 Pan evaporation estimation and derivation of explicit optimized equations by novel hybrid meta-heuristic ANN based methods in different climates of Iran. *Computers and Electronics in Agriculture* **173**, 105418.
Shammout, M. A. W., Qtaishat, T., Rawabdeh, H. & Shatanawi, M. 2018 Improving water use efficiency under deficit irrigation in the Jordan Valley. *Sustainability* **10** (11), 4317.
Song, C., Sheng, Y., Zhan, S., Wang, J., Ke, L. & Liu, K. 2020 Impact of amplified evaporation due to lake expansion on the water budget across the inner Tibetan Plateau. *International Journal of Climatology* **40** (4), 2091–2105.
Stephens, C. M., McVicar, T. R., Johnson, F. M. & Marshall, L. A. 2018 Revisiting pan evaporation trends in Australia a decade on. *Geophysical Research Letters* **45** (20), 11–164.
Trabert, W. 1896 Neue beobachtungen über verdampfungsgeschwindigkeiten. *Meteorologische Zeitschrift* **13**, 261–263.
Vlăduţ, A. Ş. & Licurici, M. 2020 Aridity conditions within the region of Oltenia (Romania) from 1961 to 2015. *Theoretical and Applied Climatology* **140** (1), 589–602.
Xu, C.-Y. & Singh, V. P. 2002 Cross comparison of empirical equations for calculating potential evapotranspiration with data from Switzerland. *Water Resources Management* **16**, 197–219.
Yamaç, S. S. 2021 Reference evapotranspiration estimation with kNN and ANN models using different climate input combinations in the semi-arid environment. *Journal of Agricultural Sciences* **27** (2), 129–137.
Yaseen, Z. M., Al-Juboori, A. M., Beyaztas, U., Al-Ansari, N., Chau, K. W., Qi, C., Ali, M., Salih, S. Q. & Shahid, S. 2020 Prediction of evaporation in arid and semi-arid regions: A comparative study using different machine learning models. *Engineering Applications of Computational Fluid Mechanics* **14** (1), 70–89.
Zarei, A. R. & Mahmoudi, M. R. 2021 Evaluation and comparison of the effectiveness rate of the various meteorological parameters on UNEP aridity index using backward multiple ridge regression. *Water Resources Management* **35** (1), 159–177.
Zhang, K., Su, Y. & Yang, R. 2019 Variation of soil organic carbon, nitrogen, and phosphorus stoichiometry and biogeographic factors across the desert ecosystem of Hexi Corridor, northwestern China. *Journal of Soils and Sediments* **19** (1), 49–57.

First received 16 November 2022; accepted in revised form 24 October 2023. Available online 28 December 2023